DOI: 10.1002/ejic.200800070

Crystal Structure, Electronic Structure, and Solid-State Electrochemistry of Cluster Complexes of $M_3Se_7^{4+}$ (M = Mo, W) with Noninnocent *o*-Phenanthroline and Se_2^{2-} Ligands

Artyom L. Gushchin,[a,b] Maxim N. Sokolov,*[a,b] Eugenia V. Peresypkina,[a] Alexandr V. Virovets,[a] Svetlana G. Kozlova,[a,b,c] Nina F. Zakharchuk,[a] and Vladimir P. Fedin*[a,b]

Keywords: Molybdenum / Tungsten / Chalcogens / Cyclic voltammetry / Electronic structure

The crystal, molecular, and electronic structure as well as the electrochemical behavior of *o*-phenanthroline complexes $[M_3Se_7(o\text{-phen})_3]X_4$ (M = Mo, W; X = Cl, Br) were investigated. Recrystallization of $[Mo_3Se_7(o\text{-phen})_3]Br_4$ from concentrated hydrochloric acid gave crystals corresponding to $[Mo_3(\mu_3\text{-Se})(\mu_2\text{-Se}_2)_3(o\text{-phen})_3]Cl_4\cdot 12H_2O$, for which X-ray analysis was performed. The bromide is isostructural. Solid-state cyclic voltammetry shows that $[M_3Se_7(o\text{-phen})_3]Br_4$ (M = Mo, W) undergoes reversible three-electron reduction, which is phen-centered with strong delocalization on the metal. DFT calculations for $\{[Mo_3Se_7(o\text{-phen})_3]Br\}^{3+}$, $[Mo_3Se_7(o\text{-phen})_3]^{4+}$, and $\{[Mo_3Se_7(o\text{-phen})_3]Br\}^0$ support the correct formulation of the reduction process. Strong interactions between the Cl^- or Br^- and Se_2 ligands of the M_3Se_7 cluster, observed in the crystal, can be described as donor–acceptor covalent bonding and are important enough to influence the redox behavior of the cluster.

Introduction

Transition-metal complexes of *o*-phenanthroline and its derivatives are of interest due to their ability to switch to long-living excited states brought about by metal-to-ligand charge transfer (MLCT). These transitions in first approximation can be treated as an electron transfer from the metal d orbital on ligand π* orbitals. *ortho*-Phenanthroline (*o*-phen) and its analogs possess two available molecular orbitals (MOs) [LUMO (b_1) and (a_2) LUMO+1] with a small energy gap between them, according to ESR studies on the $phen^{\cdot-}$[1] radical anion. Time-dependent DFT calculations for $[W(CO)_4(phen)]$ show two low-energy MLCT transitions: $W(d_\pi)\rightarrow phen(b_1)$ at 1.14 eV and $W(d_\pi)\rightarrow phen(a_2)$ at 1.21 eV[2]. One-electron reduction of $[Re(CO)_3Cl(L)]^+$ and $[Re(CO)_3(4\text{-Mepy})(L)]^+$ (L = *o*-phen; 4,7-diphenyl- and 3,4,7,8-tetramethylsubstituted phenanthrolines) was interpreted as being of the phen→$phen^{\cdot-}$ type.[3] Raman spectroscopy was used to identify $phen^{\cdot-}$ in the $[Ru(phen)_2(phen^{\cdot-})]^+$ radical complex, which was obtained by electrolysis of $[Ru(phen)_3](PF_6)_2$, and in $[Li(phen^{\cdot-})]$, which is obtained by reduction of phen with metallic Li.[4]

Coordination of the phen ligand to a cluster core is expected to lead to ambiguous electronic behavior upon reduction, as the clusters are generally regarded as electron reservoirs. More specifically, of interest to us is the redox behavior of chalcogenide clusters coordinated to phen. Among them, those with bridging dichalcogenide ligands are of particular interest, because three alternative reduction paths − metal centered, dichalcogenide centered, and phen centered − are expected to compete. In this work, we report the crystal structure, electronic structure, and electrochemistry of $[M_3(\mu_3\text{-Se})(\mu_2\text{-Se}_2)_3(o\text{-phen})_3]^{4+}$ (M = Mo, W) triangular cluster complexes.

Results and Discussion

Synthesis

Reaction of $M_3Se_7Br_4$ coordination polymers with an excess amount of *o*-phen in melt (250 °C) was shown to give $[M_3Se_7(o\text{-phen})_3]Br_4$,[5] which was not structurally characterized. In this work we managed to obtained X-ray-quality single crystals of $[Mo_3(\mu_3\text{-Se})(\mu_2\text{-Se}_2)_3(o\text{-phen})_3]Cl_4\cdot 12H_2O$ by slow cooling of a $[Mo_3Se_7(o\text{-phen})_3]Br_4$ solution in concentrated HCl. Crystallization from concentrated HBr gave single crystals of the corresponding bromide, but their poor quality prevented data collection.

[a] Nikolayev Institute of Inorganic Chemistry, Russian Academy of Sciences,
630090 Novosibirsk, Prospekt Lavrentyeva, 3, Russian Federation
[b] Novosibirsk State University,
630090 Novosibirsk, ulitsa Pirogova, 2, Russian Federation
[c] Boreskov Institute of Catalysis, Russian Academy of Sciences,
630090 Novosibirsk, Prospekt Lavrentyeva, 5, Russian Federation
Fax: +7-383-3349490
E-mail: cluster@che.nsk.su

Structure

The $[Mo_3(\mu_3\text{-}Se)(\mu_2\text{-}Se_2)_3(o\text{-phen})_3]^{4+}$ cluster cation is shown in Figure 1a. The $\{Mo_3Se_7\}$ cluster core has its usual geometry[6] (Table 1), in which each Mo atom is coordinated to one μ_3-Se (Se1), two μ-Se_2 bridges (Se2–Se3), and one chelating *o*-phen ligand. The phen ligands are all symmetry related. One of the most salient features of the $\{M_3Q_7\}^{4+}$ clusters is their high tendency to form specific bonding interactions $Q(Q_2)\cdots X$ (X = Cl, Br, I, Q = S, Se, Te) of two types: axial (Se2) and equatorial (Se3).[6–8] In the axial interactions of this cluster family, which occur almost without exception, the three chalcogen atoms of the Q_2 ligand, Q_{ax} ($3Q_{ax}\cdots X$) lying outside the Mo_3 plane (in our case, Se2; Figure 1b) participate. More than 100 structures of the M_3Q_7 clusters are currently known, but only three feature $3Se_{ax}\cdots Cl$ contacts, namely $[Mo_3Se_7\{Se_2P(iPr)_2\}_3]Cl$,[9] $[Mo_3SSe_6\{S_2P(OEt)_2\}_3]Cl$,[10] and $[W_3S_3Se_4\{S_2P(iPr_2)\}_3]Cl$.[11] These contacts fall between 2.80 (shortest) and 3.07 (longest) Å. The equatorial interactions (in our case, Se3···Cl) are less frequent and relatively longer. The Q_{ax}–$Q_{eq}\cdots X$ angles lie at 144–178° and are independent from the specific Q and X. For example, in $[Mo_3Se_7\{S_2P(iPr_2)\}_3]Cl$ the $Se_{eq}\cdots Cl$ distance is 3.03 Å and the Se_{ax}–$Se_{eq}\cdots Cl$ angle is 170.0°.[9]

The structure of $[Mo_3(\mu_3\text{-}Se)(\mu_2\text{-}Se_2)_3(o\text{-phen})_3]Cl_4\cdot 12H_2O$ features both equatorial and axial bonding interactions (Table 1, Figure 1a), whose geometry fits well into the statistics of bond lengths and angles for these clusters.[12] It also features additional contacts Se(2)···Cl(2) of 3.515(4) Å (Figure 1b, Table 1), which fall short of the (Se + Cl) van der Waals radii sum (3.7 Å). By means of all these interactions, a pair of $[Mo_3(\mu_3\text{-}Se)(\mu_2\text{-}Se_2)_3(o\text{-phen})_3]^{4+}$ cluster cations combines into the neutral $\{[Mo_3(\mu_3\text{-}Se)(\mu_2\text{-}Se_2)_3(o\text{-phen})_3]_2Cl_8\}$ linear associate (Figure 1b), in which the two constituent clusters are rotated around a $\bar{3}$ axis by 18°. These associates further form primitive cubic packing. The sandwich-like association of the type $\{M_3Q_7^{4+}\}_2X$ (X = Se^{2-}, Cl^-, Br^-) with six axial short contacts Q–Q···X was found in several structures, but it was always a bent sandwich that was formed, and the angle between the X anion and the centers of two Mo_3 triangles is 123–145°. The present structure furnishes the first example of a nonbent sandwich association (Figure 1b), with strictly perpendicular Mo_3 planes, as is imposed by crystallographic symmetry. It seems that three additional contacts Se···Cl···Se (Figure 1b), which can be achieved only when the $\{M_3\}$ planes are parallel, hinder bending. The same structural features must be attributed to the isostructural bromide salt.

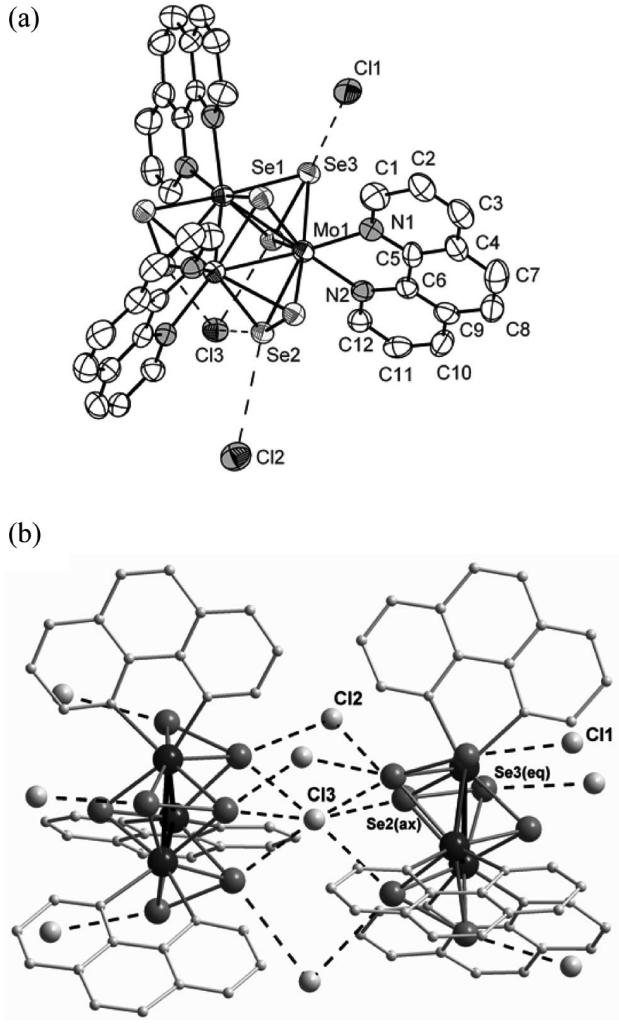

Figure 1. Atomic numbering scheme in $[Mo_3(\mu_3\text{-}Se)(\mu_2\text{-}Se_2)_3(o\text{-phen})_3]Cl_4\cdot 12(1)H_2O$ (with 50% probability ellipsoids) (a) and in $\{[Mo_3(\mu_3\text{-}Se)(\mu_2\text{-}Se_2)_3(o\text{-phen})_3]_2Cl_8\}$ (b). Dotted lines show the Se···Cl contacts. The Cl1* atoms statistically occupy 4 out of 6 symmetry related positions.

Table 1. Main bond lengths [Å] and angles [°] in $[Mo_3(\mu_3\text{-}Se)(\mu_2\text{-}Se_2)_3(o\text{-phen})_3]Cl_4\cdot 12H_2O$.[a]

Bond	Distance	Bond	Distance
Mo1–Mo1[1]	2.803(2)	Se2–Se3[2]	2.3168(18)
Mo1–Se1	2.475(2)	Mo1–N2	2.227(11)
Mo1–Se2	2.5333(17)	Mo1–N1	2.237(11)
Mo1–Se2[1]	2.5388(17)	Cl1[b]···Se3	3.057(5)
Mo1–Se3	2.6092(18)	Cl2···Se2	3.515(4)
Mo1–Se3[2]	2.6109(18)	Cl3···Se2	3.0069(11)
Angle		Angle	
Se2–Se3···Cl1[b]	165.23(6)	Cl3···Se2–Se3	168.5(1)
Cl2···Se2–Se3	106.89(5)		

[a] Atoms multiplied by symmetry codes 1: $-y + 1$, $x - y + 1$, z; 2: $-x + y$, $-x + 1$, z. [b] Statistical position occupancy is 2/3.

Electrochemistry

Half-wave cathodic ($E^c_{1/2}$ = –0.086 V) and anodic ($E^a_{1/2}$ = –0.086 V) potentials in the cyclic voltammogram (Figure 2) give evidence of a fully reversible electron exchange in solid $[Mo_3(\mu_3\text{-}Se)(\mu_2\text{-}Se_2)_3(o\text{-phen})_3]Br_4$. With the increase in scan rate (υ) from 25 to 300 mV s^{-1} the half-wave potential ($E_{p/2c}$) shifts toward more negative values, and with an approximation reliability of 0.997, the following regression equation applies: $E_{p/2c} = 0.0205\log\upsilon - 0.045$. According to Brainina,[13] fully reversible electrode processes

satisfy the equation $dE/d\log v = 0.059/n$. By applying this equation, we calculated the number of electrons transferred in the electrochemical process as 2.88, which can be interpreted as a three-electron reduction of the cluster complex.

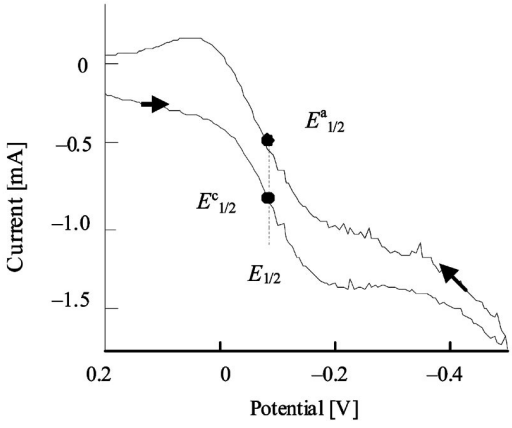

Figure 2. Cyclic voltammogram of solid $[Mo_3(\mu_3\text{-}Se)(\mu_2\text{-}Se_2)_3(o\text{-phen})_3]Br_4$ immobilized on a graphite electrode. Scan route: 0.2 → –0.6 → 0.2 V. Scan rate 0.1 $V s^{-1}$.

The cyclic voltammogram of the $[W_3(\mu_3\text{-}Se)(\mu_2\text{-}Se_2)_3(o\text{-phen})_3]Br_4$ tungsten cluster obtained under the same experimental conditions features cathodic and anodic half-wave potentials at –0.60 and –0.65 V, respectively. Thus, going from Mo to W shifts the half-wave potential by –0.51 V, which is consistent with metal-centered reduction or with strong delocalization over both π* orbitals of phen and the d orbitals of M. This situation is intermediate between two limiting cases – $[Mo_3Se_7(o\text{-phen}^{-})_3]Br$ and $\{[M^{III}_3Se_7(o\text{-phen})_3]Br\}$. This conclusion is also supported by quantum chemical calculations of $\{[Mo_3Se_7(o\text{-phen})_3]Br\}^{3+}$ (vide infra). They show the possibility to accommodate three electrons on the 15A2 and 60E1 (LUMO+1) orbitals (Figure 3) with comparable contributions from the 4d Mo and 2p C atomic orbitals (AOs).

This is the first example of reversible reduction of the $\{M_3Q_7\}^{4+}$ clusters. Although electrochemical behavior of the M_3Se_7 clusters was not reported, the sulfide analogs are known to undergo irreversible six-electron reduction with elimination of three S^{2-} and formation of the very stable incomplete cuboidal cluster core $\{Mo_3S_4\}^{4+}$.[14]

Electronic Structure

To assess the possibility of an electron going on specific ligand/metal-centered orbitals upon reduction we have calculated the electronic structure of $\{[Mo_3Se_7(o\text{-phen})_3]Br\}^{3+}$ (**I**) and of its reduced form $\{[Mo_3Se_7(o\text{-phen})_3]Br\}^{0}$ (**II**). We used bromide in the calculations, because the electrochemistry was studied for the bromide salt. The coordinates were taken from the experimental data for isostructural chloride in the C_{3v} point group. The optimized geometries for **I** and **II** are given in Table 2. Optimized interatomic distances in **I** are in agreement with the crystallographic data (Tables 2 and 3). Figures 3 and 4 show the MO energy levels in **I** and **II** and their frontier orbitals. The doubly degenerate 59E1 orbital is predominantly composed of a 4d Mo AO for both **I** (HOMO) and **II** (HOMO-2). The Mo–Mo and Mo–Se_2 interactions are bonding and the Mo–N interactions are antibonding. The 14A2 orbital (HOMO-1) is mainly carbon-based (2p C 80%). The nondegenerate 15A2 orbital (LUMO in **I**, HOMO-1 in **II**) is predominantly Mo based in **I**, and it has a greatly increased contribution from the carbon AO in **II**. The Mo–Mo interactions here are antibonding, whereas both the Mo–Se_2 and Mo–N combinations are bonding. These HOMO and LUMO compositions agree qualitatively well with earlier calculations for $\{Mo_3S_7\}^{4+}$.[15] The doubly degenerate 60E1 orbital (LUMO+1) in **I** is mainly an equal combination of the 4d Mo and 4p Se AOs. In **II**, the 60E1 orbital becomes the HOMO with an increased contribution from the carbon-centered AO, which becomes more important than participation of Mo-, Se-, or N-based AOs (Figures 3 and 4). This orbital is Mo–Mo antibonding and corresponds to a mixture of bonding and antibonding between Mo and Se_2^{2-} and between Mo and μ_3-Se. Thus, upon reduction, the three electrons must pass upon the 15A2 and doubly degenerate 60E1 levels, which all have comparable contributions from the 4d Mo AO and from the 2p C AO (corresponding to the π* orbitals of phenanthroline). The contribution from

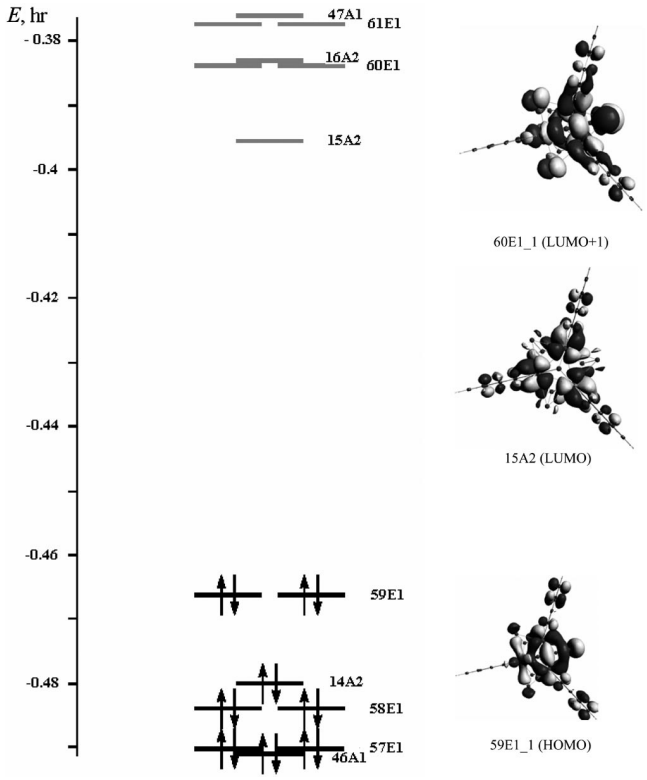

Figure 3. MO energy levels of $\{[Mo_3S_7(o\text{-phen})_3]Br\}^{3+}$ (**I**) and view of the HOMO and LUMO. Orbital compositions: 59E1: 4d Mo 52%, 4p Se 19%, 2p C 21%, 2p N 2%; 15A2: 4d Mo 62%, 4p Se 13%, 2p C 18%, 2p N 5%; 60E1: 4d Mo 41%, 4p Se 41%, 2p C 10%, 2p N 4%.

the metal orbitals explains the strong negative shift in $E_{1/2}$ that is observed on going from the Mo to the W cluster (Mo as a 4d element is more electronegative than W, a 5d element). As a consequence, the placement of one electron upon the 60E1 orbital upon three-electron reduction of **I** must have a Jahn–Teller distortion. In accordance with the Mo–Mo antibonding character of the 15A2 (HOMO-1) and 60E1 (HOMO) orbitals in **II**, reduction causes elongation and thus weakening of the Mo–Mo bonds (by about 0.2 Å). From all these calculations it follows that three-electron reduction must lead to the $[M_3^{IV}Se_7(o\text{-phen}^-)_3]^+$ state as a product, with strong delocalization of the electron density from phen$^-$ to M.

Table 2. Optimized calculated values of interatomic distances [Å] for $\{[Mo_3S_7(o\text{-phen})_3]Br\}^{3+}$ (**I**) and $\{[Mo_3S_7(o\text{-phen})_3]Br\}^{0}$ (**II**).

	Mo–Mo	Mo–Se	Mo-μ_3-Se	Se–Se	Se–Br	Mo–N
I	2.862	2.582	2.535	2.386	2.971	2.286
		2.662				2.289
II	3.022	2.605	2.690	2.388	3.074	2.186
		2.690				2.212

Table 3. Characteristics of (bcp) critical point: ρ is the electron density [e a^{-3}], $\nabla^2\rho$ is the electron density Laplacian [e a^{-5}], G, U, and E are the densities of kinetic, potential, and full energy, respectively [h a^{-3}], G/ρ is the ratio of kinetic energy density to the electron density (1 h = 27.2 eV, a = 0.529 Å, e = elementary charge).

	ρ	$\nabla^2\rho$	G	U	E	G/ρ
I	0.031	0.054	0.016	–0.019	–0.003	0.508
II	0.025	0.049	0.013	–0.014	–0.001	0.520

To understand the nature of the Se_{ax}–Br interaction and its possible influence on the redox behavior of the cluster we applied the topological approach of Bader to the $\{[Mo_3S_7(o\text{-phen})_3]Br\}^{3+}$ (**I**) complex.[16] This revealed the presence of a bond critical point (bcp) of a (3,–1) type between Se and Br at 1.548 Å from Br and 1.423 Å from Se, with a Br–bcp–Se angle of 179.3°. Critical saddle point parameters are given in Table 3. The cumulative experience gained in dealing with the properties of bcp's and, in particular, the analysis of chalcogen–halogen interactions,[17] has allowed us to describe the axial Se···Br interaction as close to a covalent one. The saddle point location outside the Se–Br vector indicates a stress in the bonding, which is a feature of covalent bonding only. For the reduced $\{[Mo_3S_7(o\text{-phen})_3]Br\}^{0}$ (**II**) complex, the bcp lies at 1.519 Å from Br and at 1.453 Å from Se with a Br–bcp–Se angle of 176.6°. The full energy density on going from **I** to **II** becomes almost zero, a fact that indicates greatly reduced Se–Br covalent bonding in **II**. This seems to be a consequence of increased electron density upon Se_2 in the reduced complex, which weakens its acceptor properties. These results agree qualitatively with the previous calculations of the $(\{Mo_3S_7\}X)^{3+}$ systems (X = Cl$^-$, Br$^-$, I$^-$), which also point to an essentially covalent nature of this interaction.[15]

NBO analysis on the level of second order perturbation theory allowed us to describe this interaction as donor–acceptor bonding between Br$^-$ and Se_2^{2-} (more precisely, do-

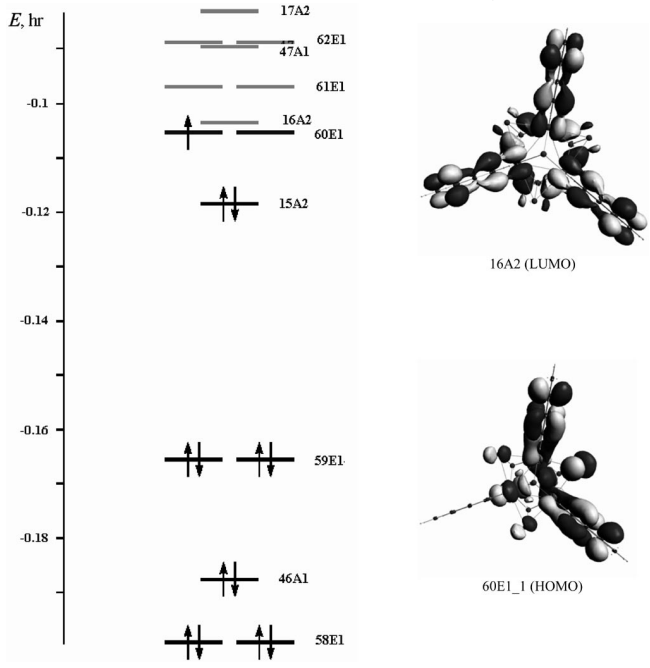

Figure 4. MO energy levels of $\{[Mo_3S_7(o\text{-phen})_3]Br\}^{0}$ (**II**) and view of the HOMO and LUMO. Orbital compositions: 59E1: 4d Mo 63%, 4p Se 17%, 2p C 13%; 15A2: 4d Mo 36%, 4p Se 7%, 2p C 42%, 2p N 13%; 60E1: 4d Mo 21%, 4p Se 17%, 2p C 43%, 2p N 17%.

nation from Br sp_y, p_z, sp_x lone-pair orbitals to the σ* orbital of the Se_2^{2-} ligand, rather like in the complexes of dihalogens, X_2·L or in I_3^-). It is worthwhile to point out that the Q_2^{2-} dichalogenide ions (present as ligands here) are isoelectronic with neutral dihalogen molecules.

Table 4 summarizes calculated atomic charges in **I** and **II**. According to the calculations, Br bears a small negative charge, which does not contradict the covalent nature of the Se–Br bonding. The increase in the absolute charge value on Br in **II** is in agreement with a drop in covalency of the Se–Br interaction on going from **I** to **II**.

Table 4. Calculated atomic charges in $\{[Mo_3S_7(o\text{-phen})_3]Br\}^{3+}$ (**I**) and $\{[Mo_3S_7(o\text{-phen})_3]Br\}^{0}$ (**II**) (in electron charge units).

	Mo	Se	μ_3-Se	Br	N
I	0.245	0.076	–0.053	–0.140	–0.099
		0.107			–0.093
II	0.221	–0.035	–0.131	–0.299	–0.117
		0.037			–0.112

To assess a possible influence of the Se_2···Br coordination upon redox properties, we also performed calculations on the $[Mo_3Se_7(phen)_3]^{4+}$ cluster by neglecting the Se···Br contacts. In that case, the HOMO and LUMO compositions alter dramatically: the HOMO is mainly (70% 2p C), whereas LUMO and LUMO+1 are mainly Se_2 based (4p Se 80%, LUMO) and Mo based (4d Mo, 78%). It follows that in the absence of a Se···Br interaction the reduction would be primarily Se centered, which would lead to the $[Mo^{IV}_2Mo^{III}(Se_2^{3-})_2(Se^{2-})(o\text{-phen})_3]^+$ state, with reduced

diselenides (Se_2^{2-} + e = Se_2^{3-}), with no participation of the phen π* orbitals. This can be interpreted as a competition between two acceptor levels, the π* orbitals of phen and the σ* orbitals of Se_2^{2-}, for electronic density. Coordination of Br^- to Se_{ax}. allows only one mode of reduction − to populate the phen π* levels.

To summarize, the first example of reversible reduction of $\{M_3Q_7\}^{4+}$ cluster complexes was found in this study. The cluster can be reduced in the solid state, and the reduction is a three-electron process. At the same time, it was shown that specific $Q_2\cdots X$ axial interactions can assume essentially covalent character and are of enough strength to change the nature of the HOMO and LUMO and the reduction pattern of the cluster molecule.

Experimental Section

Materials: The phenanthroline $[M_3Se_7(o\text{-phen})_3]Br_4$ complexes were synthesized as described previously.[5] Single crystals of dodecahydrates $[Mo_3(\mu_3\text{-Se})(\mu_2\text{-Se}_2)_3(o\text{-phen})_3]X_4\cdot 12H_2O$ (X = Cl, Br) were grown by slow evaporation of $[M_3Se_7(o\text{-phen})_3]Br_4$ solutions in concentrated HCl and HBr, respectively. They easily lose the water of crystallization once removed from the mother liquor.

Electrochemistry: As the complexes are soluble only in concentrated acids and it was thought that proton reduction would dominate the CVA picture in such media, the electrochemical behavior was studied by the method of immobilized solid particles.[18] The cyclic voltammograms were recorded with a 797 VA Computrance setting (Metrohm, Switzerland). A 10-mL, three-electrode cell was employed. As main electrode, a polyethylene and paraffin-impregnated graphite with immobilized solid particles of the complexes under investigation were used. Immobilization was achieved by rubbing crushed crystals of the complexes into the end surface of the graphite electrode. More details concerning electrode preparation are to be found in refs.[19,20] An Ag/AgCl reference electrode, filled with 3 M KCl, was used, and the auxiliary electrode was a Pt wire (6.0343 Metrohm). The background electrolyte was 0.1 M Na_2SO_4, which was prepared by dissolving sodium sulfate (puriss.) in redistilled water.

Quantum Chemical Calculations: Calculations of the electronic structure was carried out for model complexes $\{[Mo_3S_7(o\text{-phen})_3]Br\}^{3+}$ (**I**) and $\{[Mo_3S_7(o\text{-phen})_3]Br\}^{0}$ (**II**) (both C_{3v}) by using the ADF 2005 program package,[21] which included a program for NBO analysis.[22] Geometry optimization was achieved by using spin-restricted DFT, in which model Hamiltonians of density functional were represented as the sum of local density functional LDA (VWN[23]) and gradient exchange functional GGA (Becke[24] & Perdew[25]). As basis wavefunctions, Slater orbitals (ADF/TZP) with core potentials of (1s.3d) for Mo, (1s.3p) for Se, (1s.3d) for Br, (1s) for N, and (1s) for C were used. Atomic charges were calculated by the Hirshfeld method.[26] Analysis of critical saddle points was done by using the "Atoms in Molecule" approach[16] and by using the Xaim software developed by Jose Carlos Ortiz and Carles Bo, Universitat Rovira i Virgili, Tarragona, Spain.

X-ray Structure Determination: The structure of $[Mo_3(\mu_3\text{-Se})(\mu_2\text{-Se}_2)_3(o\text{-phen})_3]Cl_4\cdot 12H_2O$ was determined by single-crystal X-ray analysis. The crystals have a strong tendency for twinning. Diffraction data were obtained with a four-circle automatic diffractometer Bruker X8APEX with a two coordinate CCD detector; Mo-K_α (λ = 0.71073 Å) radiation; graphite monochromator. Crystallographic data and experimental details are given in Table 5. Empirical absorption correction was applied from equivalent reflections intensities by using the SADABS program.[27] The structure was solved by direct method and refined with full-matrix least-squares method anisotropically (for non-hydrogen atoms) with the SHELXTL program package.[28] All the molecules of water of crystallization, except one, are disordered. The multiplicities of the positions of the oxygen atoms in the water molecules were first refined with fixed thermal parameters and then kept as calculated. If the position multiplicity was less than 0.5, isotropic refinement was applied. The estimated error in hydrate number determination from combined uncertainty in calculating the multiplicities of the positions occupied by oxygen atoms is about $1H_2O$ per formula unit. Main bond lengths are given in Table 1. The bromide $[Mo_3(\mu_3\text{-Se})(\mu_2\text{-Se}_2)_3(o\text{-phen})_3]Br_4\cdot\approx 12H_2O$ is isostructural with the chloride [a = 21.6612(9) Å, c = 55.730(5) Å]. CCDC-675096 contains the supplementary crystallographic data for this paper. These data can be obtained free of charge from The Cambridge Crystallographic Data Centre via www.ccdc.cam.ac.uk/data_request/cif.

Table 5. Crystallographic data and experimental details for $[Mo_3(\mu_3\text{-Se})(\mu_2\text{-Se}_2)_3(o\text{-phen})_3]Cl_4\cdot 12H_2O$.

Formula	$C_{36}H_{47.70}Cl_4Mo_3N_6O_{11.85}Se_7$
Molecular weight	1736.44
Temperature	150.0(2)
Crystal system	Trigonal
Space group	$\bar{R}3c$
a [Å]	21.3781(3)
c [Å]	55.1487(13)
V [Å^3]	21827.5(7)
Z	12
$\rho_{calcd.}$ [g cm^{-3}]	1.585
μ [mm^{-1}]	4.202
$2\theta_{max}$ [°]	50
Number of measured/independent/ observed [$I > 2\sigma(I)$] reflections, R_{int}	42041/4265/2746 0.1010
Number of refined parameters	236
R_1 [$I > 2\sigma(I)$]	0.0703
wR_2 (all data)	0.2482
Residual electron density (max/ min)	3.012/–0.767

Acknowledgments

The work was financially supported by the Russian Foundation for Basic Research (grant 05-03-32126) and through a Presidential Grant to M. N. S (MD-7072.2006.3), by a grant from the Russian Science Support Foundation to A. L. G, and by the Presidium of the Siberian Branch of the Russian Academy of Sciences through a Lavrentyev Grant to E. V. P. We thank Mr. A. I. Smolentsev for diffraction data collection and Carles Bo for his kind help with the Xaim program.

[1] W. Kaim, *J. Am. Chem. Soc.* **1982**, *104*, 3833–3837.
[2] I. R. Farrell, J. van Slageren, S. Zalis, A. Vlcek, *Inorg. Chim. Acta* **2001**, *315*, 44–52.
[3] S. L. Howell, K. C. Gordon, *J. Phys. Chem. A* **2006**, *110*, 4880–4887.
[4] J. R. Schoonover, K. M. Omberg, J. A. Moss, S. Bernhard, V. J. Malueg, W. H. Woodruff, T. J. Meyer, *Inorg. Chem.* **1998**, *37*, 2585–2587.
[5] V. P. Fedin, M. N. Sokolov, O. A. Gerasko, A. V. Virovets, N. V. Podberezskaya, V. Ye Fedorov, *Inorg. Chim. Acta* **1991**, *187*, 81–90.

[6] A. V. Virovets, A. L. Gushchin, P. A. Abramov, N. I. Alferova, M. N. Sokolov, V. P. Fedin, *Zh. Strukt. Khim.* **2006**, *47*, 332–345.
[7] A. V. Virovets, N. V. Podberezskaya, *Zh. Strukt. Khim.* **1993**, *34*, 150–160.
[8] M. N. Sokolov, P. A. Abramov, A. L. Gushchin, I. V. Kalinina, D. Y. Naumov, A. V. Virovets, E. V. Peresypkina, C. Vicent, R. Llusar, V. P. Fedin, *Inorg. Chem.* **2005**, *44*, 8116–8124.
[9] C. W. Liu, C.-S. Fang, C.-W. Chuang, T. S. Lobana, B.-J. Liaw, J.-C. Wang, *J. Organomet. Chem.* **2007**, *692*, 1726–1734.
[10] J. Hu, H.-H. Zhuang, S.-X. Liu, J.-L. Huang, *Transition Met. Chem.* **1998**, *23*, 547–557.
[11] R. Hernandez-Molina, M. Sokolov, P. Nunez, A. Mederos, *J. Chem. Soc., Dalton Trans.* **2002**, 1072–1077.
[12] a) J.-H. Liao, J. Li, M. G. Kanatzidis, *Inorg. Chem.* **1995**, *34*, 2658; b) M. J. Almond, M. G. B. Drew, H. Redman, D. A. Rice, *Polyhedron* **2000**, *19*, 2127–2133; c) M. D. Meienberger, K. Hegetschweiler, H. Ruegger, V. Gramlich, *Inorg. Chim. Acta* **1993**, *213*, 157–169; d) H.-P. Zhu, Q.-T. Liu, C.-N. Chen, Y.-H. Deng, *Jiegou Huaxue* **1998**, *17*, 142–152; e) L. Xianti, H. Jianquan, H. Jinling, *Jiegou Huaxue* **1985**, *4*, 143–153; f) X.-T. Lin, J.-X. Lu, J.-L. Huang, J.-Q. Huang, *Jiegou Huaxue* **1990**, *9*, 236–244; H. Liao, M. G. Kanatzidis, *Inorg. Chem.* **1992**, *31*, 431–439.
[13] Kh. Z. Brainina, *Stripping Voltammetry in Chemical Analysis*, Haisted Press, New York, **1974**, p. 222.
[14] K. Hegetschweiler, T. Keller, W. Amrein, W. Schneider, *Inorg. Chem.* **1991**, *30*, 873.
[15] M. J. Mayor-Lopez, J. Weber, K. Hegetschweiler, M. Meienberger, F. Joho, S. Leoni, R. Nesper, G. J. Reiss, W. Frank, B. A. Kolesov, V. P. Fedin, V. E. Fedorov, *Inorg. Chem.* **1998**, *37*, 2633–2644.
[16] R. F. Bader, *Atoms in Molecules: A Quantum Theory*, Clarendon, New York, **1990**.
[17] V. A. Slepkov, S. G. Kozlova, S. P. Gabuda, V. E. Fedorov, *THEOCHEM* **2008**, *849*, 112–212.
[18] F. Scholz, B. Meyer, "Voltammetry of Solid Microparticles Immobilized on Electrode Surfaces" in *Electroanalytical Chemistry: A Series of Advances* (Eds.: A. J. Bard, I. Rubenstein), Dekker, New York, **1998**, vol. 20, pp. 1–86.
[19] F. Scholz, B. Meyer, *Chem. Soc. Rev.* **1994**, *23*, 341–347.
[20] N. Zakharchuk, B. Meyer, H. Hennig, F. Scholz, A. Jaworksi, Z. Stojek, *J. Electroanal. Chem.* **1995**, *398*, 23–33.
[21] *Amsterdam Density Functional (ADF) Program*, Release 2005.02, Vrije Universteit, Amsterdam, The Netherlands, **2005**.
[22] E. D. Glendening, J. K. Badenhoop, A. E. Reed, J. E. Carpenter, J. A. Bohmann, C. M. Morales, F. Weinhold, *NBO 5.0*, Theoretical Chemistry Institute, University of Wisconsin, Madison, **2001**.
[23] S. H. Vosko, L. Wilk, M. Nusair, *Can. J. Phys.* **1980**, *58*, 1200–1205.
[24] A. D. Becke, *Phys. Rev. A* **1988**, *38*, 3098–4008.
[25] J. P. Perdew, *Phys. Rev. B* **1986**, *33*, 8822–8832.
[26] L. Hirshfeld, *Theor. Chim. Acta* **1977**, *44*, 129–139.
[27] *APEX2* (version 1.08), *SAINT* (version 7.03), and *SADABS* (version 2.11), Bruker Advanced X-ray Solutions, Bruker AXS Inc., Madison, Wisconsin, USA, **2004**.
[28] *SHELXTL* (version 6.12), Bruker Advanced X-ray Solutions, Bruker AXS Inc., Madison, Wisconsin, USA, **2004**.

Received: January 22, 2008
Published Online: July 25, 2008

